ORIGINAL PAPER

Irrigation efficiency optimization at multiple stakeholders' levels based on remote sensing data and energy water balance modelling

Chiara Corbari[1] · Marco Mancini[1]

Abstract

The agricultural sector, the largest and least efficient water user, is facing important challenges in sustaining food production and careful water use. The objective of this study is to improve farm and irrigation district water use efficiency by developing an operational procedure for smart irrigation and optimizing the exact water use and relative water productivity. The SIM (smart irrigation monitoring and forecasting) optimization irrigation strategy, based on soil moisture (SM) and crop stress thresholds, was implemented in the Chiese (North Italy) and Capitanata (South Italy) Irrigation Consortia. The system is based on the energy–water balance model FEST-EWB (Flashflood Event-based Spatially distributed rainfall runoff Transformation Energy–Water Balance model), which was pixelwise calibrated with remotely sensed land surface temperature (LST), with mean areal absolute errors of approximately 3 °C, and then validated against local measured SM and latent heat flux (LE) with RMSE values of approximately 0.07 and 40 Wm^{-2}, respectively. The effect of the optimization strategy was evaluated on the reductions in irrigation volume and on the different timing, from approximately 500 mm over the crop season in the Capitanata area to approximately 1000 mm in the Chiese district, as well as on cumulated drainage and ET fluxes. The irrigation water use efficiency (IWUE) indicator appears to be higher when applying the SIM strategy than when applying the traditional irrigation strategy: greater than 35% for the tomato fields in southern Italy and 80% for maize fields in northern Italy.

Introduction

Agriculture is the largest consumer of water worldwide, accounting for 24% of total freshwater uses in Europe, with peaks of 80% in the southern regions (Zucaro 2014; FAO 2018), while irrigation is one of the sectors where there is one of the largest differences between modern technologies and largely diffused ancient traditional practices (Singh and Singh 2017). Climate change and increasing human pressure (Ingram 2011) together with traditional wasteful irrigation practices are enhancing the conflictual problems in water use, also in countries traditionally rich in water (Wada et al. 2011). The improvement of irrigation efficiency is a fundamental step for achieving sustainable food and water, security and safety (Alexandratos et al. 2012).

Although this issue is becoming more common every year, for a long time, several techniques have been developed in the research community to improve irrigation management, mainly based on the use of agro-hydrological modelling coupled with ground information and always with more satellite data (Calera Belmonte et al. 2017; Bastiaanssen et al. 2000; Prueger et al. 2018; Knipper et al. 2019; Corbari et al. 2019a) for either monitoring vegetation status or providing the land surface temperature (LST) for controlling evapotranspiration. Recently, these models have often been coupled with new low-cost ground sensor networks (Navarro-Hellín et al. 2015), and they have been further improved by their combined use with meteorological forecasts to predict irrigation water needs (Cao et al. 2019; Lorite et al. 2015; Cabelguenne et al. 1997; Pelosi et al. 2016; Ceppi et al. 2014).

These models are then used to drive improved irrigation strategies, which may regulate irrigation volumes and timing by considering the potential evapotranspiration (D'Urso 2010; Calera Belmonte et al. 2005; Toureiro et al. 2017; Xu et al. 2019), soil moisture (SM) threshold (Allen et al. 1998; Steduto et al. 2009) or deficit irrigation (Comas et al. 2019; Brown et al. 2010; Geerts and Raes 2009), while also considering saline and fresh water (Acosta-Motos et al. 2017).

✉ Chiara Corbari
chiara.corbari@polimi.it

1   Politecnico di Milano, Piazza Leonardo da Vinci 32,
    20133 Milan, Italy

Moreover, some authors, such as Farré and Faci (2009), have also shown that no changes in crop yield may be found if less irrigation is provided than the potential ET.

The effect of these improved irrigation strategies may be evaluated by means of efficiency indicators, such as the mostly diffused water use efficiency (WUE) or the irrigation water use efficiency (IWUE), which consider crop production over ET or irrigation amounts, respectively. Zwart et al. (2010) performed a comprehensive review of WUE and IWUE over the globe, which was then revised by Bastiaanssen and Steduto (2017). Additionally, other indicators are available based on water losses due to the percolation flux or soil degradation (Hatfield and Dold 2019; Koech and Langat 2018).

Hence, the main objective of this study is the optimization of irrigation management by increasing the IWUE (e.g., decreasing the amount of water used while maintaining the same crop productivity) at both the Irrigation Consortium and field scales across Italy. Intermediate objectives can then be defined: (1) to calibrate and validate the hydrological model at both scales against ground and satellite information, (2) to implement the irrigation optimization strategy and (3) to evaluate its potential in terms of water savings. The analyses are performed with the energy–water balance model FEST-EWB (Flashflood Event-based Spatially distributed rainfall runoff Transformation Energy–Water Balance model), which is pixel-wise calibrated with LST remote sensing data and validated against local measurements of soil moisture and evapotranspiration data (Corbari et al. 2011). The FEST-EWB model has previously been demonstrated to be able to accurately simulate ET and SM at the local scale against eddy covariance station measurements (Corbari et al. 2011), as well as at the irrigation consortium scale in comparison to satellite land surface temperature data considering irrigation distribution (Corbari et al. 2013, 2020) and at the catchment scale against remotely sensed LST and river discharge in the Po and Yangtze River basins (Corbari and Mancini 2014; Corbari et al. 2019b). The FEST-EWB model has also been used for smart irrigation management combined with remote sensing data and meteorological forecasting in an asparagus field in southern Italy (Corbari et al. 2019a).

The optimization irrigation strategy, SIM (smart irrigation monitoring and forecasting) (Mancini et al. 2021), was developed based on soil moisture crop stress thresholds, allowing the triggering of irrigation only when needed in any field in the consortium area. The effects of the newly implemented strategy are finally evaluated on the irrigation volumes, the cumulated drainage and the evapotranspiration fluxes.

The methodology is applied in two case studies: the Chiese and Capitanata Irrigation Consortia, which are located in northern and southern Italy, respectively. These areas mainly differ in terms of climatic conditions, crop types, irrigation strategies and techniques.

With respect to previous studies, the main innovative aspects of this study are (1) the implementation of an optimized irrigation management strategy not only at the local scale but for any field in the irrigation consortium area; (2) the importance of the regional study across different Italian irrigation consortia for improving the actual inefficient irrigation practices; and (3) the extensive validation of the FEST-EWB model at several eddy covariance stations to prove its robustness after its pixelwise calibration against satellite LST.

Materials and methods

Case studies

Two case studies, indicative of Italian agriculture, were selected to demonstrate the potential for water-saving applications: the Capitanata (southern Italy) and Chiese (northern Italy) Irrigation Consortia, which have different climates, soil and crop types, water availability and source, irrigation schemes and water distribution rules. These diversities contributed to demonstrating the robustness of the analysis. The two case studies are detailed in Fig. 1.

In particular, the Capitanata Irrigation Consortium (www. consorzio.fg.it), located in the Puglia Region in southern Italy, has an area of 50,000 ha and is dedicated to intensive agriculture with two main crop seasons: spring and summer dedicated to wheat and tomatoes and autumn and winter dedicated to fresh vegetables. The climate is characterized by hot dry summers and warm wet winters. A pressurized water network pumping water from two reservoirs distributes irrigation water on demand to the fields from April to October with a mean seasonal amount of 600 mm over a precipitation average of approximately 150 mm. Daily irrigation volumes over the whole Consortium are available from 2013 to 2018. Mean annual volumes range between 2 and 6 * 10^7 m^3, depending on the year. The fields are mainly irrigated with drip and micro-sprinklers techniques.

The Chiese Irrigation Consortium (20,000 ha) (www. consorziodibonificachiese.it), located in the Lombardia Region near Lake Idro in northern Italy, is a highly irrigated area cultivated with summer crops, such as maize and forage and winter wheat. The irrigation is supplied through a dense channel network of 1400 km based on a priori fixed irrigation turn every 7 ½ to 8 ½ days from April to September. The surface irrigation technique is the most diffuse, with a mean turn volume of approximately 100 mm. Over the crop season, a mean rainfall value of 250 mm is present, while the average irrigation is 1200 mm.
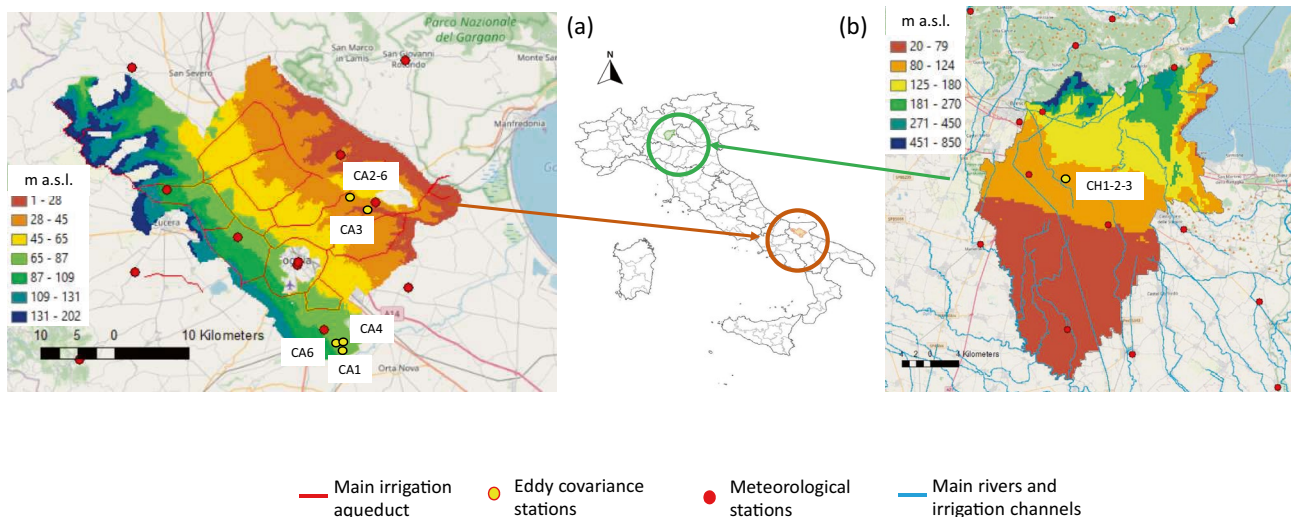
Fig. 1 The Capitanata (**a**) and Chiese (**b**) Irrigation Consortia and their position within Italy. The meteorological stations and the eddy covariance sites are highlighted in both case studies, along with the main irrigation aqueduct in the Capitanata area and the main irrigation channels network in the Chiese area

Meteorological data

For the Capitanata area, 21 meteorological stations managed by the official Puglia Region ARPA network and by the private association Meteonetwork (Fig. 1) provided measurements of precipitation, air temperature and relative humidity, incoming solar radiation and wind speed at an hourly time stamp from 2013 to 2018. The same dataset is also available for the Chiese area, where 15 stations are managed by the ARPA Lombardia, Regione Trentino and Meteonetwork association. These data are available from 2005 to 2018.

Evapotranspiration and soil moisture data

Eddy covariance stations were installed in different fields in both case studies (Fig. 1) to measure evapotranspiration, sensible heat flux, net radiation and soil moisture. In particular, soil moisture measurements were performed with TDR (Time Domain Reflectometer) soil moisture sensors (CS616, Campbell Sci, UT, USA) at different soil depths, which were representative of the maximum density of crop roots: approximately 15 cm from fresh vegetables and at 35 cm for maize (Lundstrom and Stegman, 1988). A three-dimensional sonic anemometer (Young 81,000 by Campbell Scientific) and a gas analyser (LI-COR 7500) were installed at the top of the stations (2.5 m in the fresh vegetables and 5.5 m in the maize) to measure the CO_2 and H_2O concentrations in the atmosphere. A radiometer (CNR 1 by Kipp and Zonen) was mounted on top of the stations to measure the four components of net radiation. The soil ground heat flux was measured with two thermocouples and a heat flux plate (HFP01 by Hukseflux) at a depth of 10 cm.

PEC software (Polimi Eddy Covariance) (Corbari et al. 2012) was applied to correct the turbulent fluxes according to the main instrumental and physical correction procedures (Foken 2008). Moreover, latent and sensible heat fluxes usually underestimate the available energy, leading to a non-closure of the energy balance (Masseroni et al. 2014). Hence, these fluxes were modified according to the procedure developed by Twine et al. 2000 based on the preservation of the Bowen ratio method to reach the energy budget closure. Last, eddy covariance turbulent fluxes were measured over a source area, which was computed with the two-dimensional footprint model of Detto et al. (2006). Hence, FEST-EWB estimates of latent and sensible heat fluxes were also integrated as a weighted sum over the footprint area to be consistent with measured values (Detto et al. 2006):

$$\overline{F} = \frac{\sum_{i=1}^{n} f\left(x_i, y_i, z_m\right) F\left(x_i, y_i\right)}{\sum_{i=1}^{n} f\left(x_i, y_i, z_m\right)} \tag{1}$$

where i is the position of a pixel in an image, F is the flux value in each pixel, $\overline{F}$ is the average flux in the footprint area, f is the footprint dimension, x is the footprint in the upwind direction and y in the orthogonal direction, and z_m is the height of measurement.

In the Capitanata area, six seasons of eddy covariance data are available between 2016 and 2018 covering different crops and soil types (Table 1): Stations CA1 and CA2 in two tomato fields during 2016 in a silty clay and sandy soil, respectively; Station CA3 in a tomato field during 2017; in a field where wheat (Station CA5) was sowed until 2018;

Table 1 Case studies fields, with soil type, planting/sowing and harvesting dates, crop type

Crop type	Short name	Soil type	Planting/sowing	Harvesting
Capitanata				
Tomatoes	CA1	Silty clay	23 May 2016	8 September 2016
Tomatoes	CA2	Sandy	12 May 2016	28 august 2016
Tomatoes	CA3	Silty loam	20 April 2017	1 August 2017
Asparagus	CA4	Silty clay loam	1 December 2013	15 September 2014*
Wheat	CA5	Silty loam	11 November 2017	9 June 2018
Cabbage	CA6	Sandy	30 August 2016	2 February 2017
Chiese				
Maize	CH1	Sandy loam	4 May 2016	7 September 2016
Maize	CH2		15 April 2017	23 August 2017
Maize	CH3		6 April 2018	1 September 2018

*The date does not refer to crop harvesting but to station dismounting

Station CA4 with pluri-annual crop asparagus from 2013 to 2014; and Station CA6 in a cabbage field during 2016 (Corbari et al. 2020). Instead, in the Chiese Consortium, data from a single eddy covariance station are available between April and September from 2016 (CH1), 2017 (CH2) and 2018 (CH3) (Table 1). For all analysed fields, the dates of the irrigation events and water volumes are known.

Soil type and crop data

Soil characteristics are accessible from the regional datasets of Regione Puglia (http://www.sit.puglia.it/portal/sit_portal) for the Capitanata Consortium and of Regione Lombardia (http://www.cartografia.regione.lombardia.it/rlregisdownload/) for the Chiese Consortium. Information on the different soil classes, according to the USDA triangle, allowed us to define the soil hydraulic properties according to Rawls and Brakensiek (1985), which were then used as input in the FEST-EWB model. The active soil depth involved in the water cycle computation, which was relevant for the evapotranspiration process, was initially set to be equal to 0.5 m in the Capitanata Consortium, which is representative of the root development zone of the most diffuse fresh vegetables in the area, while a value of 1.2 m in the Chiese Consortium was significant for maize roots.

Crop yield data at field stations are available from farmers' data for tomato fields in Capitanata Consoritum and for maize fields in the Chiese area. In addition, a global dataset is available for both areas from the ISTAT database (http://dati.istat.it/).

Remote sensing data

Multiple satellite data (from MODIS, Landsat 7 and 8, and Sentinel 2) were used either as input data in the hydrological model (vegetation fraction (fv), leaf area index (LAI) and albedo) and for calibration and validation (land surface temperature (LST)).

For the two Consortia areas, data at different spatial resolutions were used, relying on the hypotheses that the mean field dimensions in the Capitanata area are well reproduced by a 30 m pixel dimension, which was further reinforced by the presence of a large variety of crop types, while for the Pianura Padana plain, (where the Chiese basin is located), characterized by highly homogeneous maize cultivated areas, lower-resolution data from MODIS at 250 m to 1 km were able to detect this low variability among the vegetated areas. Corbari et al. (2015) reported a mean difference of 1.2 °C among LST images at 250 m and at 1 km.

For the Capitanata Consortium, the data were processed from 2013 to 2018 with Landsat 7 and Landsat 8 data available every 16 days (63 and 67 images, respectively), while Sentinel 2 data were processed every ten days (40 images), as described in Corbari et al. (2020). All images were atmospherically corrected with 6S (Landsat-8 case) or Sen2Corr (Sentinel-2 case) software to estimate the bottom of atmosphere reflectance. The vegetation indices were computed from Sentinel 2 and Landsat 7 and 8 satellite images at 30 m spatial resolution following the procedure implemented in Corbari et al. (2020): the vegetation fraction was computed as in Gutman and Ignatov (1998), while LAI was computed as a function of fv and the light extinction coefficient (Choudhury 1987).

LST was computed from Landsat 7 and 8, as described by Skokovic (2017) and Skokovic et al. (2017), using the Single Channel and Split Window algorithms, respectively (Jimenez-Munoz et al. 2014). Then, a sharpening process was carried out to bring the resolution from 100 m (Landsat 8) and 60 m (Landsat 7) to 30 m using the Nearest Neighbor Temperature Sharpening (NNTS). The method takes into account similar pixel properties and their distance, both over a sliding N×N window over an LST image, using relationships of Normalised Difference Water Index (NDWI) and

Normalised Difference Vegetation Index (NDVI) indices versus the LST. The reliability of the remotely sensed LST was analysed in comparison with ground measurements performed at the location of the eddy covariance stations, providing a mean absolute error close to zero and an RMSE of 3.0 K and R^2 value of 0.88 and an RMSE of 2.0 K and R^2 value of 0.92 for ETM + and TIRS estimates, respectively (Corbari et al. 2020).

For the Chiese study area, MODIS satellite data (http://ladsweb.nascom.nasa.gov/index.html) were analysed from 2005 to 2016 for both vegetation indices and LST, retrieving 3965 images. The leaf area index was retrieved from the MOD15A2–leaf area index product generated over an 8-day compositing period (Myneni et al. 2002), while the albedo maps were retrieved from the MODIS white-sky product over an 8-day compositing period at 5 km (Liang 2001). LST products from the MODIS/Terra LST/E Daily L3 Global 1-km Grid product (MOD11A1) were downloaded with a spatial resolution of 1 km and a daily temporal resolution. A downscaling methodology was then adopted to improve the spatial resolution to 500 m, following the disaggregation procedure for radiometric surface temperature (DisTrad)

based on a regression between NDVI (at high- and low-spatial resolution) and LST (Kustas et al. 2003).

Methodology

The methodology (Fig. 2) that was implemented may be divided into two main steps: (1) step 1 refers to the calibration and validation of the hydrological model, and (2) step 2 refers to the implementation of the irrigation strategy. In particular, satellite data of LST and point-scale measurements of soil moisture and evapotranspiration were used for the calibration and validation of the FEST-EWB model. The optimized SIM irrigation strategy was then executed based on soil moisture thresholds, and finally, different efficiency indicators were determined to quantify the impact of the SIM strategy.

FEST-EWB model

The FEST-EWB (Flashflood Event-based Spatially distributed rainfall runoff Transformation Energy–Water Balance model) is a distributed land surface energy–water balance
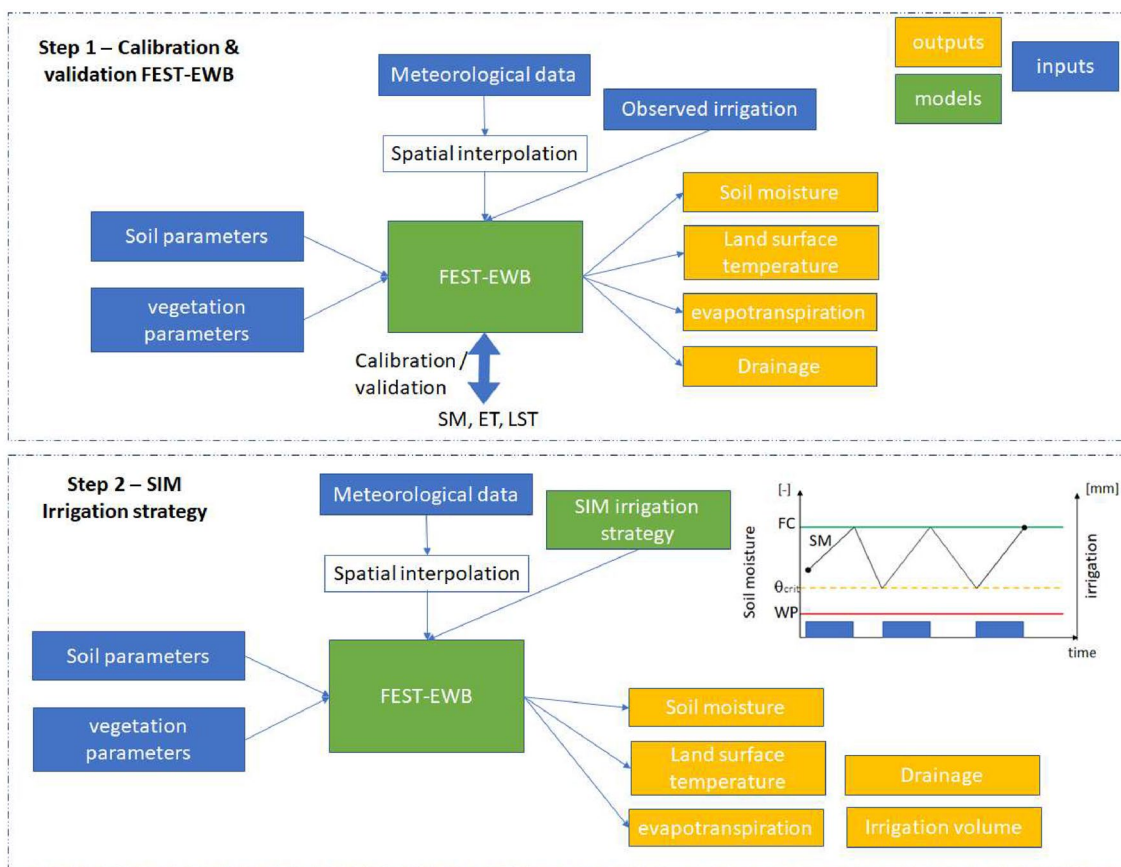

Fig. 2 The paper methodology: (1) step 1—calibration and validation of the hydrological model, (2) step 2—implementation of the irrigation strategy. For each step the input data, model and outputs are highlighted

model (Corbari et al. 2011; Mancini 1990) that computes all the main processes of the water-land surface cycle.

FEST-EWB resolves the system of the energy and water budgets equations in each pixel of the analysed area, searching for the representative equilibrium temperature (RET) as the land surface temperature that allows the energy balance equation to be closed. The two energy and water balances equations are then connected by the evapotranspiration flux. The system is calculated as:

$$\begin{cases} \frac{\partial SM_{i,j}}{\partial t} = \frac{1}{dz_{i,j}}\left(P_{i,j} - R_{i,j} - PE_{i,j} - ET_{i,j}\right) \\ Rn_{i,j} - G_{i,j} - H_{i,j} - LE_{i,j} = 0 \end{cases} \tag{2}$$

where $\frac{\partial SM_{i,j}}{\partial t}$ is soil moisture over time (-), $P_{i,j}$ is the precipitation rate (mm h^{-1}), $R_{i,j}$ is the runoff flux (mm h^{-1}), $PE_{i,j}$ is the drainage flux (mm h^{-1}), $ET_{i,j}$ is the evapotranspiration rate (mm h^{-1}), d$z_{i,j}$ is the soil depth (m), $Rn_{i,j}$ (Wm^{-2}) is the net radiation, $G_{i,j}$ (Wm^{-2}) is the soil heat flux, $H_{i,j}$ (Wm^{-2}) is the sensible heat flux, $LE_{i,j}$ (Wm^{-2}) is the latent heat flux, and i and j are the pixel coordinates. Surface and subsurface river discharges are not computed, as the analysed case studies agricultural areas.

The main model input data are (1) meteorological variables, such as air temperature and relative humidity, solar radiation, wind velocity and precipitation; (2) irrigation amount; (3) soil hydraulic parameters, such as saturated hydraulic conductivity or saturated soil moisture; (4) vegetation parameters, such as leaf area index (*LAI*), vegetation fraction and minimum stomatal resistance (*rsmin*); and (5) digital elevation model and land use map.

The application of daily irrigation volumes (m^3) is performed by rescaling the volumes as mm day^{-1} of irrigation height, accounting only for the irrigated vegetable pixels. These occurrences are detected by merging the information from the area land use and satellite data of vegetation fraction, where fv > 0.05 allows separating vegetated areas from bare soil. In the Capitanata Consortium, tomatoes and plurennial asparagus, vineyard and olive trees are irrigated as spring and summer crops, while several fresh vegetables are irrigated during late August and autumn. In the Chiese area, the main irrigated crop is maize during the spring–summer period, plus some other minor crops.

Calibration and validation The FEST-EWB model was calibrated pixel by pixel, looking for the minimum difference between the simulated RET and the observed LST in each single pixel, based on the procedure developed by Corbari and Mancini (2014), where each single pixel is tuned independently from the others; then, it is validated at the local scale against soil moisture and evapotranspiration measurements. This is feasible because RET is an internal model variable directly linked to the latent and sensible heat fluxes as well as

the soil moisture condition. Hence, thanks to this approach, SM and ET are improved at the pixel scale as well as globally.

The calibration process is regulated by the pixel-by-pixel minimization of the average model error, defined as the objective function O:

$$O \underset{=}{\mathrm{def}} \frac{1}{n} \cdot \sum_{i=1}^{n} \left(RET_i - LST_i\right) \tag{3}$$

where *n* stands for the total number of calibration dates selected.

The most relevant parameters involved in the calibration process are the soil hydraulic conductivity, the soil depth, the minimum stomatal resistance, the soil evaporation resistance, the aerodynamic resistance and the Brooks–Corey index. This was verified by Corbari and Mancini (2014), who performed sensitivity analyses on all the main parameters governing the water and energy balances in the FEST-EWB model by comparing simulated energy fluxes and soil moisture with ground-measured fluxes.

A "trial and error" approach was implemented to calibrate the soil and vegetation parameters. Therefore, parameter tuning was performed by testing several combinations of parameter values step by step in the FEST-EWB model simulations, changing a single parameter or a combination of them, until the difference between RET and LST was minimized. The FEST-EWB model was initially assigned to different parameter literature-suggested values, which were in turn modified in each single pixel of a percentage that allowed the objective function to tend to zero. The parameter values were always kept within their physical ranges for each soil class (Rawls and Brakensiek 1985).

Applying this distributed calibration procedure, the traditional calibration methodology based on the comparison between modelled and observed local soil moisture or discharge data was improved, allowing us to overcome the global parameter calibration, which was usually changed using a single correction factor for the whole analysed area. Instead, the pixel-by-pixel approach of the calibration process allowed us to accurately refine the spatial heterogeneity of the calibration parameters involved for the whole consortium area.

Model robustness is quantified through the absolute mean error (MAE) and the root mean square error (RMSE), which are computed as follows:

$$MAE = \frac{\sum_{i=1}^{n} |S_i - M_i|}{n} \tag{4}$$

$$RMSE = \sqrt{\frac{\sum_{i=1}^{n} \left(S_i - M_i\right)^2}{n}} \tag{5}$$

where S_i is the ith simulated variable, M_i is the ith measured variable, n is the sample size, and $\overline{M}$ is the average observed variable. These statistical values are computed either for LST, ET and SM knowing that the lower the RMSE is, the lower the error (e.g., the same occurs for the MAE).

SIM irrigation strategy

The decision criteria of the SIM irrigation strategy rely on the comparison among the modelled soil moisture value and two crop-specific SM thresholds: the field capacity (FC), as the surplus threshold that corresponds to the SM value for which the drainage flux starts, and the crop stress threshold (θcrit), for which the crops start to suffer from a lack of water. This method allows defining both the correct irrigation timing (i.e., starting irrigation when the modelled SM becomes equal to the stress threshold) and the irrigation water amount (i.e., stopping irrigation when the modeled SM reaches the FC threshold). A scheme of this strategy is shown in Fig. 2. This SIM strategy reduces the drainage flux and, as a consequence, the water volume without impacting evapotranspiration and crop yield.

θcrit is defined as a function of the different types of soils and crops, considering their growth stage and climate (Allen et al. 1998) as:

$$\theta_{crit} = FC - p_{new} * (FC - WP) \tag{6}$$

where WP is the wilting point and p_{new} is a corrected value of p, which is computed as a fraction of the total available water (TAW) that can be depleted from the root zone. According to Allen et al. 1998, p_{new} is computed as:

$$p_{new} = p + \left(0.04 \cdot \left(5 - ET_{i,j}\right)\right) \tag{7}$$

Typical values of p range between 0.30 for crops with superficial roots at high values of ET (> 8 mm d^{-1}) and 0.70 for crops with deep roots at low ET values (< 3 mm d^{-1}). A value of 0.50 for p is commonly used for many crops. p is computed as:

$$p = \frac{RAW}{TAW} \tag{8}$$

where RAW is the readily available water, computed as the difference between FC and the stress threshold, and TAW is computed as the difference between FC and WP.

The underlying hypothesis of this methodology is that the crop yield is expected to remain constant because the soil moisture never decreases below the stress threshold (Allen et al. 1998), a limit below which evapotranspiration is limited to less than potential values.

Water efficiency indicators

To evaluate the impact of the application of the SIM irrigation strategy with respect to the traditional farmers, different water indicators were evaluated by analysing the differences in terms of crop yield and water use as well as the percolation flux. The four selected indicators are calculated as follows:

$$\text{Water use efficiency (ton/m3) : } WUE = \frac{yield}{ETv} \tag{9}$$

$$\text{Irrigation water use efficiency (ton/m3) : } IWUE = \frac{yield}{Iv} \tag{10}$$

$$\text{Percolation deficit : } P_{er}D = \frac{(P+I) - P_{er}}{P+I} \tag{11}$$

$$\text{Irrigation efficiency : } IE = \frac{ET}{P+I} \tag{12}$$

where ETv is the evapotranspiration volume (m^3 ha^{-1}), yield is the crop yield (ton ha^{-1}), Iv is the observed or modelled irrigation volume (m^3 ha^{-1}), P is precipitation (mm), I is irrigation (mm), Perc is the percolation flux (mm) and ET is evapotranspiration (mm).

Results

Model calibration and validation

Capitanata consortium

The model was extensively calibrated by Corbari et al. (2020), and here, a summary of the results is reported. The model was optimized so that the RMSE among satellite LST and FEST-EWB RET images was minimized in each single pixel independently from the other, allowing us to reach a mean value of 2.7° over the entire period (2014–2016) and area. The remotely sensed land surface temperature data for 2017 and 2018 were then used to validate the FEST-EWB model, resulting in a pixel-by-pixel MAE of 3.5 °C. In Fig. 3, the boxplot for each satellite image date is shown for both Landsat 7 and 8 satellites and FEST-EWB data, highlighting the capability of the FEST-EWB model in reproducing the observed LST with either the calibration or the validation datasets.

The application of the pixel-by-pixel calibration procedure led to soil and vegetation parameter changes in either their mean values or their spatial distribution with

Fig. 3 Boxplot for each satellite image date for satellite and FEST-EWB land surface temperature (LST) over the whole Capitanata case study area for the calibration (**a**) and validation (**b**) periods. On each box, the central mark indicates the median, and the bottom and top edges of the box indicate the 25th and 75th percentiles, respectively. The whiskers extend to the most extreme data points not considered outliers, and the outliers are plotted individually using the '+' symbol
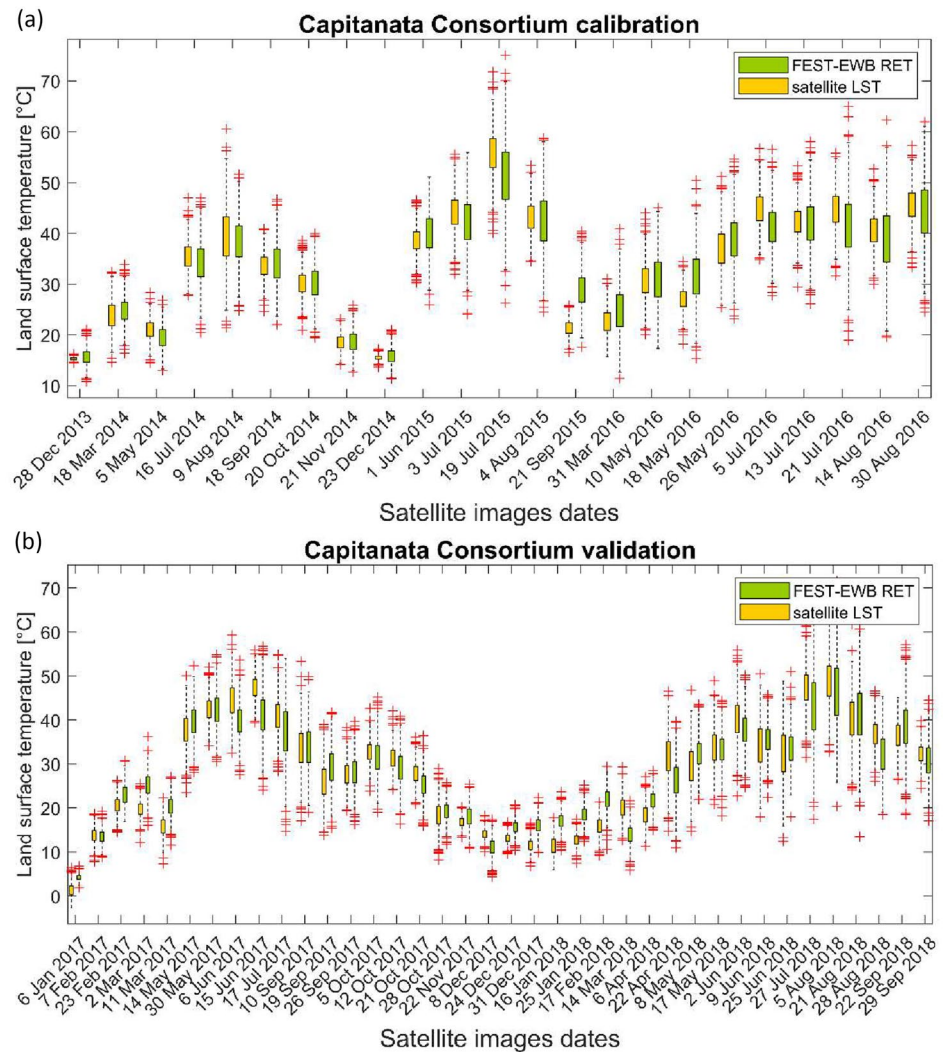
a sensible increase in the standard deviation values with respect to the values before the FEST-EWB calibration (Table 2).

SM and LE measured at the eddy covariance stations during the crop seasons were then used to validate the modelled FEST-EWB fluxes locally in each field. For each hourly time series of modelled and observed fluxes, the standard deviation ratio ($\sigma_{FEST-EWB}/\sigma_{eddy}$), the normalized Root Mean Square Difference (RMSD/σ_{eddy}) and the correlation coefficient (ρ) were computed. In Fig. 4, two Taylor plots (Taylor 2001), one for SM and one for LE, are shown to summarize all these statistical indices, showing the capability of the FEST-EWB model to also reproduce the local-scale measurements of evapotranspiration and soil moisture at each site. For the plurennial asparagus crop (CA4), the average score was quite positive for LE, with a correlation higher than 0.7 and RMSD/σ less than 0.8, and an RMSE of 33.3 W m^{-2}. Soil moisture had a correlation higher than 0.8 and an RMSD/σ less than 0.7, with an RMSE of 0.04. The

two tomato fields during 2006, CA1 and CA2, had comparable values of normalized standard deviation (~0.90) and correlation (~0.70) for LE, with RMSEs of 43 W m^{-2} and 40 W m^{-2}, respectively. For soil moisture, starting from correlation coefficients, CA1 had a very high value (0.9) and a normalized standard deviation next to 1, while CA2 had a lower correlation coefficient (0.8) and a higher RMSD/σ of approximately 1.2. A correlation coefficient of 0.8 and a normalized standard deviation higher than 0.6 were obtained for the modelled SM for the CA3 tomato field during the 2017 season. The agreement was confirmed for LE even though a lower correlation was found (0.6) with a normalized standard deviation near 1. Similar results were obtained for the wheat field (CA5) with an RMSD/σ of 0.6 on soil moisture and a normalized standard deviation next to 1 (e.g., 1 is for observation), while LE had a similar behaviour to CA3 with a normalized standard deviation and RMSD/σ both near 1 and a correlation coefficient of 0.6. Finally, for the cabbage field (CA6), high RMSE values (0.1) were obtained for soil

Table2 Mean and standard deviation (SD) values of soil hydraulic and vegetation parameters over the whole Capitanata and Chiese Consortia before and after the FEST-EWB calibration (saturated hydraulic conductivity (ksat), minimum stomatal resistance (rsmin), Brooks and Corey index (BC), field capacity (FC), WP wilting point (WP))

	Before calibration	After calibration
	Mean (SD)	Mean (SD)
Capitanata consortium		
ksat (ms^{-1})	$2.8*10^{-8}$ ($4.1*10^{-7}$)	$4.5*10^{-7}$ ($3.3*10^{-6}$)
Soil depth (m)	0.5 (0.13)	0.78 (1.3)
rsmin (sm^{-2})	40.8 (19)	75 (41.8)
BC	0.215 (0.03)	0.117 (0.04)
FC	0.48 (0.04)	0.36 (0.07)
WP	0.28 (0.04)	0.16 (0.05)
Chiese consortium		
ksat (ms^{-1})	$2.4*10^{-5}$ ($2.6*10^{-5}$)	$3.5*10^{-6}$ ($7*10^{-5}$)
Soil depth (m)	0.67 (1.4)	0.78 (1.6)
rsmin (sm^{-2})	180 (30)	139 (62)
BC	0.54 (0.24)	0.252 (0.09)
FC	0.16 (0.05)	0.27 (0.08)
WP	0.07 (0.05)	0.117 (0.08)

moisture as well as for the latent heat flux, with an RMSE of 49 W m^{-2} and a coefficient of determination of 0.7.

Chiese consortium

The differences between LST from MODIS and RET were computed iteratively for each date during the calibration process. A total of 3965 LST images from MODIS were considered, 2193 of which were used for the calibration period (2005–2011). RET estimates from FEST-EWB before calibration generally highly underestimated observed satellite values, with a mean absolute difference pixel by pixel of 5.2 °C, while after the calibration procedure, it was equal to 3.4 °C. The model was then validated for the period between 2011 and 2016, and a mean absolute difference of 2.9 °C for the irrigation district area was obtained. In Fig. 5, the boxplot for a random selection of available dates is shown for both MODIS satellite and FEST-EWB data over the calibration and validation periods, confirming the ability of the model to spatially represent land surface temperature.

In Table 2, the main soil hydraulic and vegetation parameters before and after the calibration are listed, showing an increase in the saturated hydraulic conductivity and in the soil depth and a decrease in the minimum stomatal resistance, with a generalized increase in the spatial standard deviation for all parameters.

The FEST-EWB model was then validated at the local scale by comparing the observed and simulated latent heat flux and soil moisture at the eddy covariance station during the 2016, 2017 and 2018 maize seasons. For each hourly time series of modelled and observed fluxes, the normalized standard deviation ratio ($\sigma_{FEST-EWB}/\sigma_{eddy}$), the normalized Root Mean Square Difference (RMSD/σ_{eddy}) and the correlation coefficient (ρ) were computed. The position in the Taylor plots of SM and LE time series confirmed the ability of the model to produce high-spatial resolution and continuous observed data over time (Fig. 4).

In particular, for soil moisture, the coefficient of correlation was approximately 0.6 for all three years, correctly being the same field (e.g., soil type) and the same irrigation technique, even though the normalized standard deviation was lower than 1.5 during 2017 and 2018 (CH2 and CH3, respectively), while during 2016 (CH1), it was almost near 2. During the 2016 and 2017 seasons, soil moisture was reproduced with an RMSE of 0.03, while an RMSE of 0.02 was found during 2018.

A high accuracy was obtained for the modelled latent heat flux, with a $\sigma_{FEST-EWB}/\sigma_{eddy}$ almost equal to 1 for all years, with a small difference in RMSD/σ between 0.4 and 1. Specifically, during the 2016 season, good reproduction was obtained for the latent heat fluxes, with an RMSE of 25.7 Wm^{-2}, which was confirmed during 2017 and 2018 with RMSEs of 18 Wm^{-2} and 20 Wm^{-2}, respectively.

SIM irrigation strategy

The SIM irrigation strategy was finally implemented in both case studies at the field and consortium district levels, quantifying the impact on irrigation timing and amount as well as on percolation and evapotranspiration fluxes through the water indicators.

Capitanata consortium

The SIM irrigation applications were performed considering at first the analysed tomato fields, being the most water-intensive summer crop and the most diffuse in the area. Hence, the FEST-EWB simulation runs using the observed irrigations were compared with the FEST-EWB simulations performed with the SIM irrigation strategy in Fig. 6. For the CA1 field, the two SM behaviours (e.g., modelled with observed irrigations and with the SIM ones) were sensibly different, confirming the contrasting irrigation strategy principles, particularly on high peaks and irrigation timing. Hence, a decrease in the irrigation amount of 37.5% was obtained from the SIM strategy application, with the measured volume equal to 516 mm and the SIM one to 322 mm (Table 3). The irrigation events were also reduced from 27 to 15. The lowering of the SM peaks allowed a percolation flux reduction of approximately 50%, while ET remained almost the same, as expected, and was always lower than the potential evapotranspiration (ET0) (Allen et al. 1998).
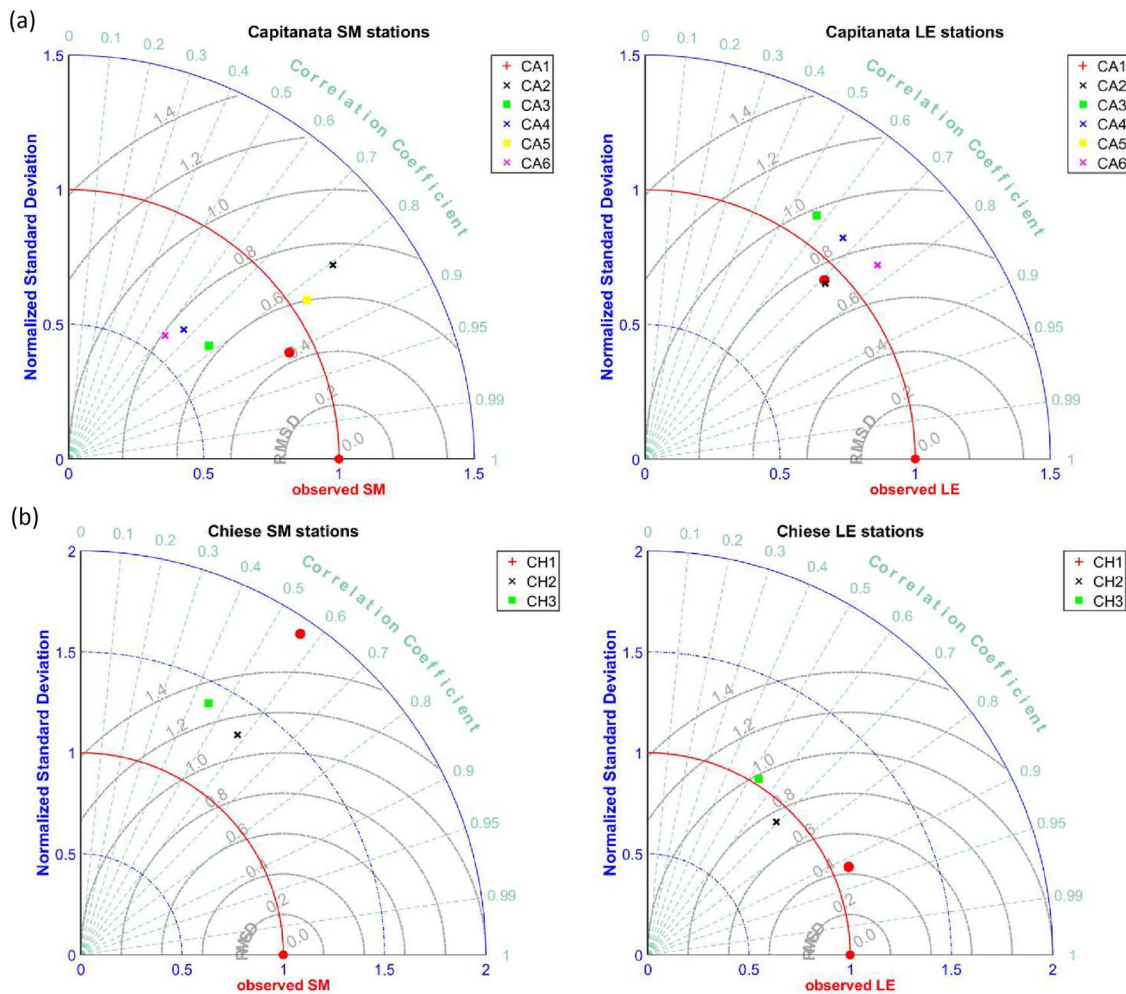
Fig. 4 Taylor plots for FEST-EWB model validation on soil moisture (SM) and latent heat flux (LE) at the different eddy covariance stations for the Capitanata (**a**) and Chiese (**b**) Consortia

In field CA2, the irrigation volume decreased from 646 to 590 mm, with a savings of 8.7% when the SIM strategy was implemented. This decrease also led to a small decrease in the drainage flux of approximately 50 mm, while the ET flux remained almost constant (Table 3). However, an increase in the number of irrigation events was observed when the SIM strategy was applied, from 43 to 90.

For field CA3, the irrigation volume was reduced by approximately 600 mm from the observed to the SIM strategy with a sensible decrease in the number of irrigation events (Table 3). As expected, the lowering of the SM peaks (Fig. 6) allowed the percolation flux reduction with the same quantity of irrigation volume to decrease, while evapotranspiration remained almost the same.

From a comparison of the overall results from the three fields, in the CA2 field, the irrigation volume decreased less than for the CA1 and CA3 fields when the SIM strategy was applied. Differences may have been due to the different

field soil types (Table 1): CA1 was characterized by silty clay soil, which had a reduced infiltration capacity compared with the CA2 sandy soil. In contrast, the decrease in irrigation events was higher for CA2 (27) than for CA1 (15), which was also relevant in irrigation management due to the implications that it might have for economic savings related to reduction in electricity or human labour costs.

Analysing each single tomato field in the whole Capitanata Consortium (Fig. 7), the measured irrigation volumes and the modelled FEST-EWB fluxes (run using the observed irrigations) were compared with the results of the modelled data from the hydrological model FEST-EWB applying the SIM strategy. The analyses were performed from the 2014 to 2018 seasons for each pixel of the irrigation consortium. The irrigation volume estimates were spatially integrated to be comparable with the observed aqueduct data. In Fig. 7, the water balance fluxes from FEST-EWB using either the observed irrigation or the SIM strategy are

Fig. 5 Box plot for some dates for satellite and FEST-EWB land surface temperature (LST) over the whole Chiese case study area for the calibration (**a**) and validation (**b**) periods. On each box, the central mark indicates the median, and the bottom and top edges of the box indicate the 25th and 75th percentiles, respectively. The whiskers extend to the most extreme data points not considered outliers, and the outliers are plotted individually using the '+' symbol
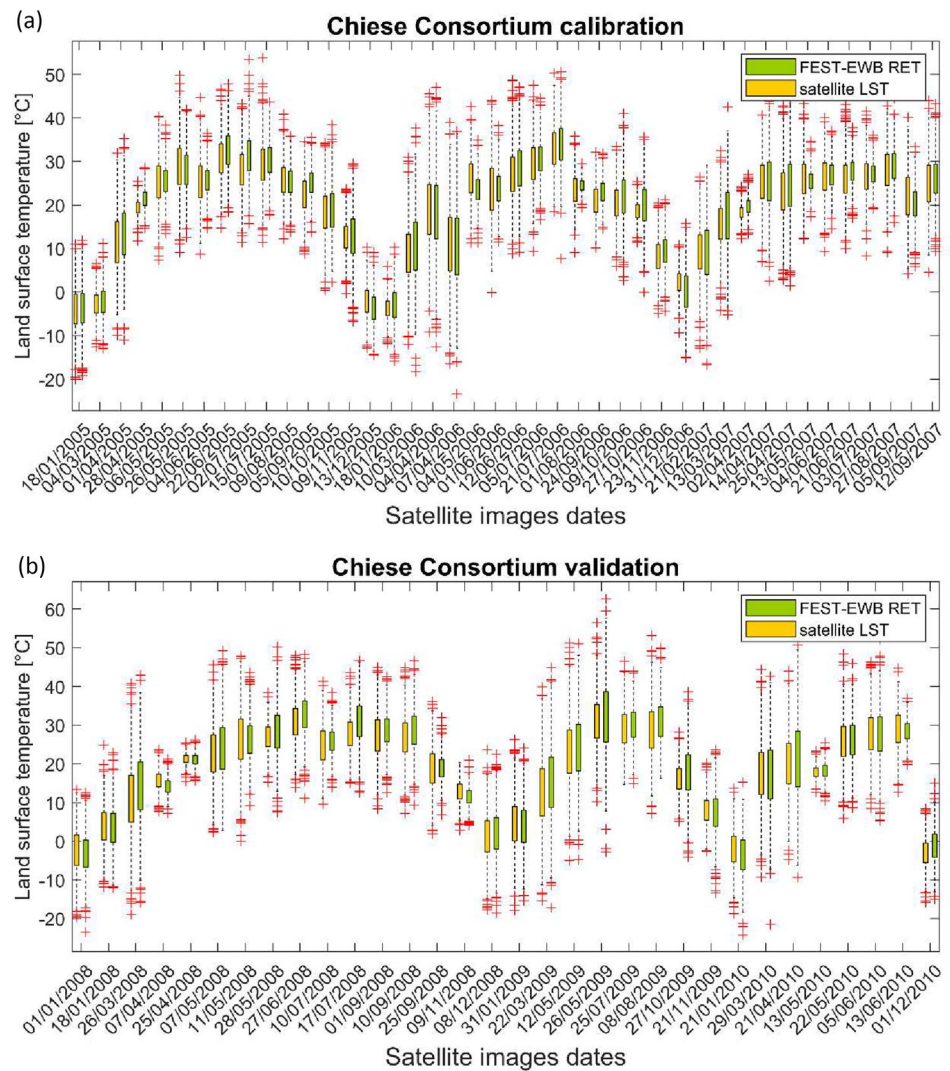
shown: precipitation, irrigation, evapotranspiration, and drainage. These results at the basin scale confirm those obtained at the field scale, with substantially similar values of evapotranspiration between the two simulation configurations and a considerable decrease in the drainage flux from the observed irrigation simulation to the SIM simulation (approximately 300 mm). The observed and SIM water demands also highlight a sensible difference, with the mean daily value over the season equal to 3.5 mm day^{-1} and to 1.4 mm day^{-1}, respectively. Hence, the SIM irrigation strategy saves approximately 500 mm of irrigation water in total in one season.

Chiese consortium

Similar to the Capitanata area, the SIM strategy was then applied to the maize fields in the Chiese Consortium. Figure 8 shows the impacts of the SIM irrigation strategy on soil moisture behaviour with respect to the moisture

interval between the FC and plant stress thresholds for the pixels of the maize control fields. In field CH1, more than 1000 mm of irrigation water volume would have been saved with the application of SIM, corresponding also to a decrease of 700 mm of the percolation flux and the relative runoff flux, while ET was slightly decreased, moving further less than the ET0 (Table 3). A different SM dynamic was obtained for the SIM strategy with respect to the observed traditional irrigation (Fig. 8), particularly its peaks, which never surpassed the field capacity threshold. The CH2 field behaved in a similar way to CH1, with a large amount of water saved when applying the SIM strategy with respect to the traditional one: more than 1000 mm with a decrease of 8 irrigation events. This was also reflected in a sensible reduction of the drainage flux by 800 mm (Table 3).

The application of the SIM strategy to the CH3 field produced similar results, with a decrease of more than 1000 mm in the irrigation water amount and number of irrigation

Fig. 6 Soil moisture dynamic and irrigation events using observed irrigations and SIM strategy for the three Capitanata tomatoes fields (CA1, CA2 and CA3). Rainfall, stress threshold and FC are also shown
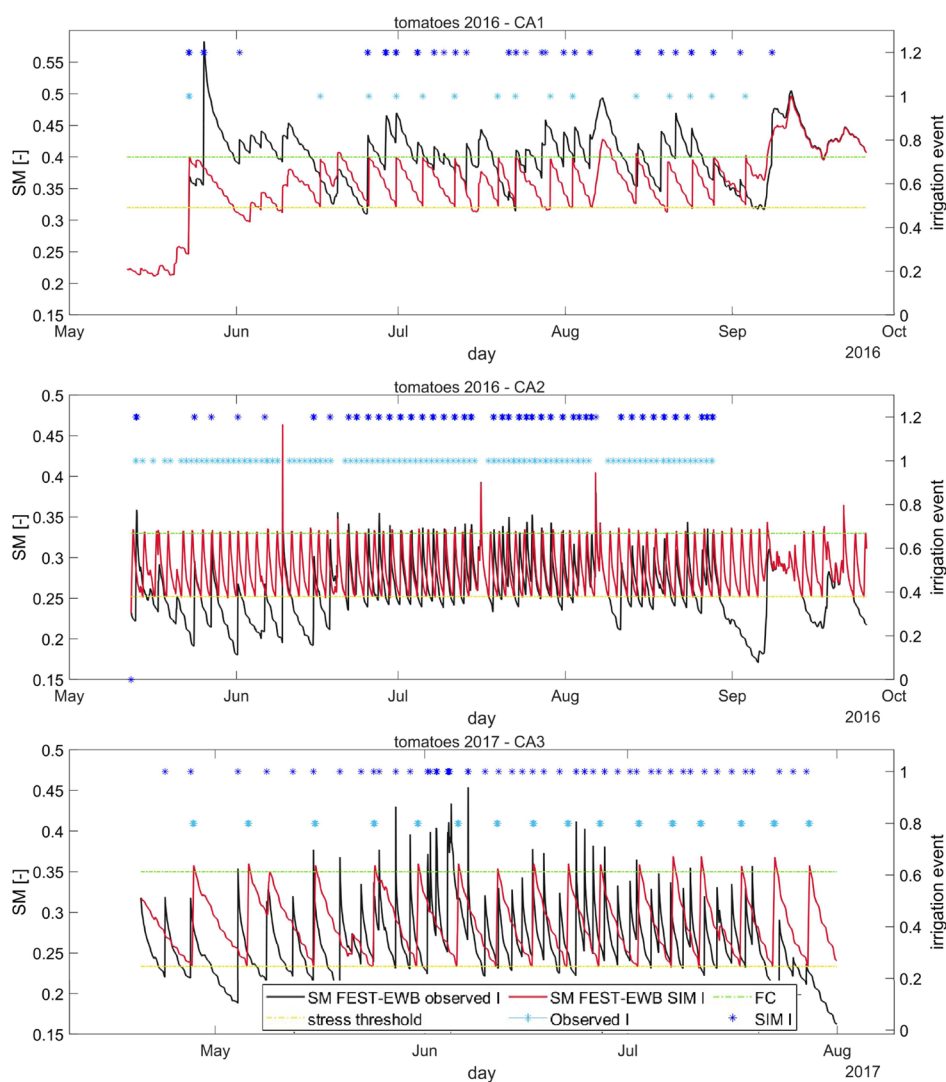

Table 3 Seasonal water fluxes from the application of the traditional and SIM irrigation strategies at field scale for both case studies

Station	Rainfall (mm)	ET0 (mm)	Observed I (mm)	Observed ET (mm)	Observed drainage (mm)	SIM I (mm)	SIM ET (mm)	SIM drainage (mm)
Capitanata								
CA1	228	725	516	450	180	322	441	80
CA2	228	718	646	280	590	590	280	235
CA3	28	420	950	260	720	321	265	110
Chiese								
CH1	214	495	1427	490	843	264	265	135
CH2	224	730	1475	580	946	490	574	143
CH3	516	570	1749	556	1210	197	550	

events (Table 3). The drainage flux also behaved in the same way, denoting a consistent reduction.

It is worth noting that the same irrigation amount was supplied to the maize field in the different seasons, even though

sensibly different precipitation amounts were observed (from 200 to 600 mm). Instead, the SIM strategy would have allowed improving the irrigation volume while also considering precipitation, weighting the two in the water cycle.

Fig. 7 Comparison of Capitanata (**a**) and Chiese (**b**) Consortia cumulated water fluxes (irrigation, ET, drainage) with observed and SIM irrigations, and rainfall
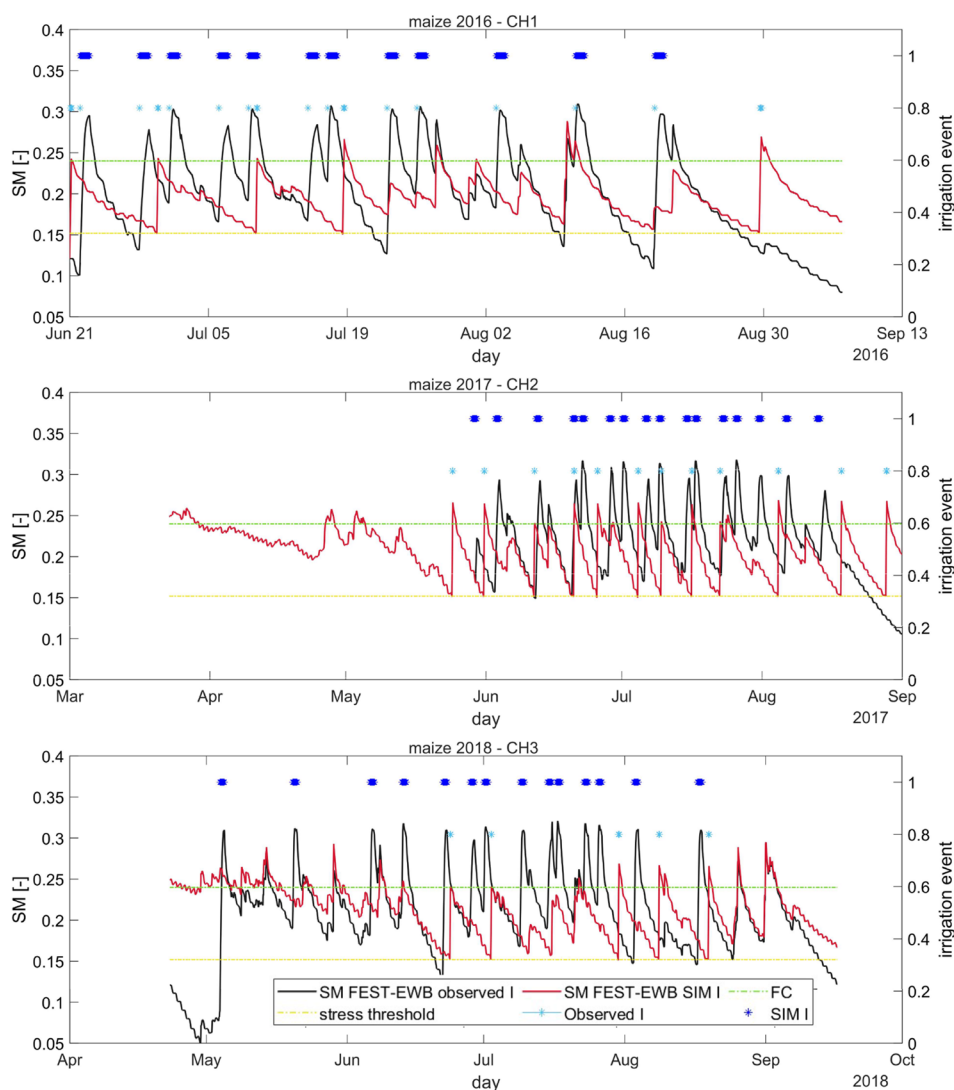
In Fig. 7, the water balance fluxes from FEST-EWB computed either for observed and SIM irrigations are shown for all maize fields in the Chiese Consortium. The results at the basin scale confirm the results obtained at the field scale with a small decrease in evapotranspiration computed with SIM irrigation with respect to the one obtained with the observed irrigation and with a halving of irrigation volume over the analysed crop seasons, leading to a considerable decrease in the drainage flux and runoff from the observed irrigation simulation to the SIM simulation (approximately 1000 mm).

Water indicators

The water efficiency indicators were finally computed at the field and consortium levels for both case studies.

Capitanata consortium

In Fig. 9, the water efficiency indicators are shown for the three tomato fields (CA1, CA2 and CA3), showing higher IWUE values, percolation deficit and irrigation efficiency when the SIM strategy was applied than when the observed irrigation was performed. The WUE indicator was instead almost constant when the two irrigation methods were compared because crop yield and evapotranspiration remained almost unchanged. These results show that an improvement in irrigation management is still feasible in the Capitanata area, where great attention to the smart use of water is already taking place due to scarce water availability. It is interesting to note the difference between the two farms, with the different soil types showing a lower efficiency for CA2 (sandy soil) than for CA1 (silty clay soil). This is also reflected in the difference
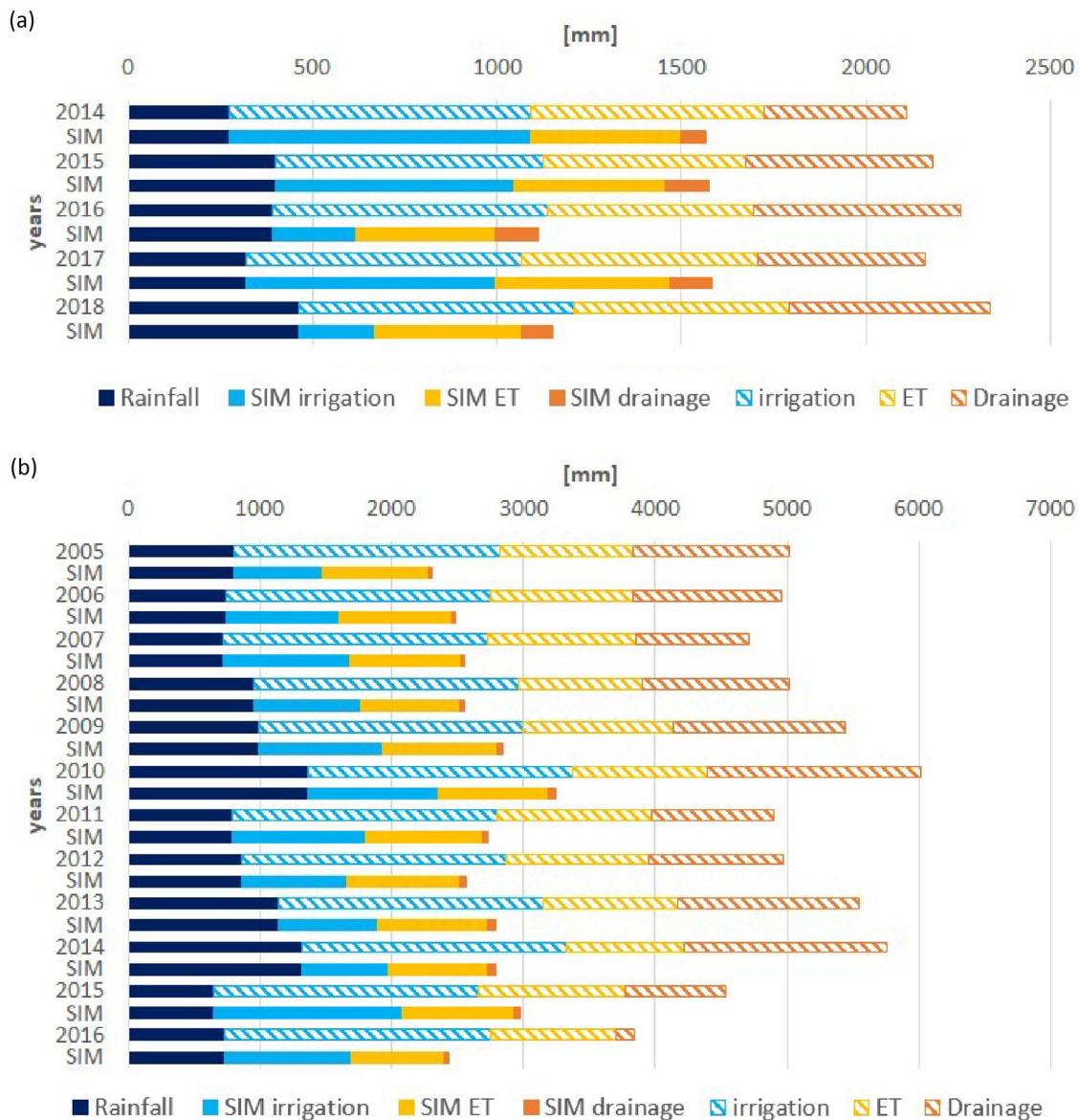
(a)

(b)

Fig. 8 Soil moisture dynamic and irrigation events using observed irrigations and SIM strategy for 2016, 2017 and 2018 Chiese maize fields (CH1, CH2, CH3). Rainfall, stress threshold and FC are also shown

between the IWUE computed with the observed irrigation and the IWUE computed with the SIM irrigation, which was equal to 14 kg m^{-3} for CA1, while for the other two fields, it was equal to 2 kg m^{-3}.

In general, the percolation deficit tended to 1 when applying the SIM strategy and was generally always higher than when the observed irrigation was applied. This was reached in most situations, except in CA3, which, as previously noted, was characterized by a highly permeable soil leading to minimum water loss even when applying the SIM strategy. This was also reflected in the irrigation efficiency indicator, which in CA3, slightly increased when using the

SIM irrigation strategy, while for CA1, the indicator reached almost the value of one.

The same indicators were then computed for the whole consortium area (Fig. 9), showing consistent values over the years as those obtained at the field scale. Hence, the WUE indicator was almost stable due to the almost constant evapotranspiration obtained from the simulation with observed or SIM irrigation, while IWUE was higher when the SIM strategy was applied, confirming the water volume savings, and the irrigation efficiency and the percolation deficit indices improved from approximately 0.5 to 0.8.
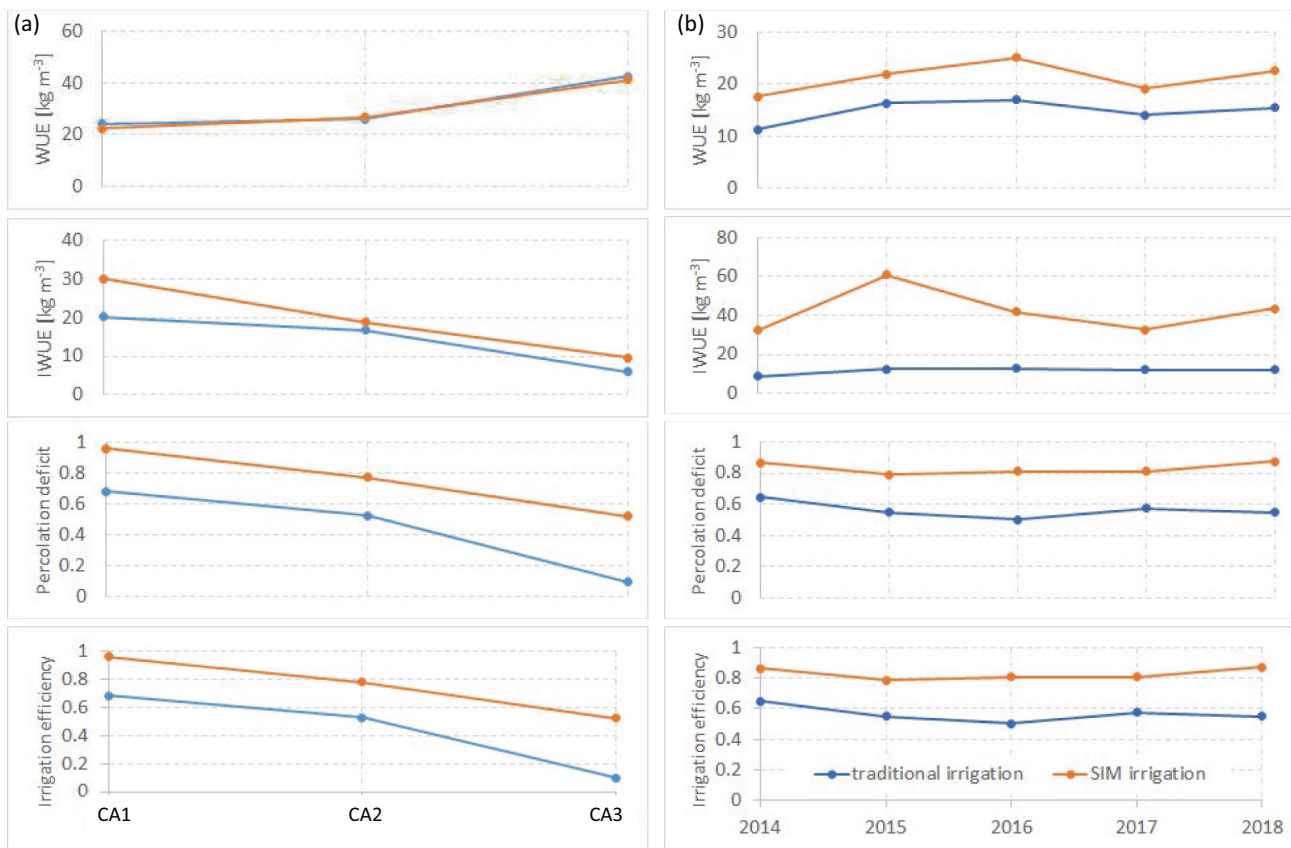
Fig. 9 Water indicators (WUE, IWUE, Percolation deficit, Irrigation efficiency) considering the observed irrigations and the SIM strategy for the analysed tomatoes fields (**a**) and for the whole Capitanata Consortium (**b**)

Chiese consortium

The water indicators were computed for the maize field over the three crop seasons in 2016, 2017 and 2018. The IWUE and percolation deficit indices were found to have higher values when the SIM strategy was applied than when traditional management was followed, with average improvements of 3.5 kg m^{-3} and 0.2, respectively. The irrigation index also showed a great improvement when the SIM methodology was implemented (approximately 0.7).

Similar results were obtained for the whole consortium area (Fig. 10). The WUE indicator was slightly greater when applying SIM irrigation, with evapotranspiration being slightly higher, while IWUE was higher, from approximately 0.5 kg m^{-3} to 1.5 kg m^{-3}, when the SIM strategy was applied, confirming the water volume savings. The irrigation efficiency and the percolation deficit indices also improved with respect to the observed irrigation strategy from approximately 0.3 to 0.57 and from 0.6 to 1, respectively.

When comparing the two case study results, similar gains in terms of IWUE were found at approximately 60%, while higher improvements in irrigation efficiency and percolation deficit were obtained for the Chiese Consortium than for the

Capitanata Consortium due to the higher amounts of water, which are traditionally used in excess in northern Italy, independent of the precipitation amount. This is mainly due to the water concessions rates, which allow paying the water at a fixed rate per year and not for the consumed water. The IE index tended to 1 if applying the SIM strategy, showing a consistent increase, especially in the Chiese Consortium, as well as the PerD index (e.g., an almost null drainage flux).

Discussion

The implemented SIM strategy may improve current irrigation practices in the operative water management of the two analysed Italian irrigation consortia, suggesting a possible review of the water distribution rules among the associates. This is due to the decrease in the irrigation volumes and number of irrigations that the farmers may implement if adopting the SIM strategy. The SIM methodology may then be used in operative water management at multiple stakeholder levels, providing an advancement with respect to several irrigation advisory services that are based on remotely sensed multispectral images for crop status classification and
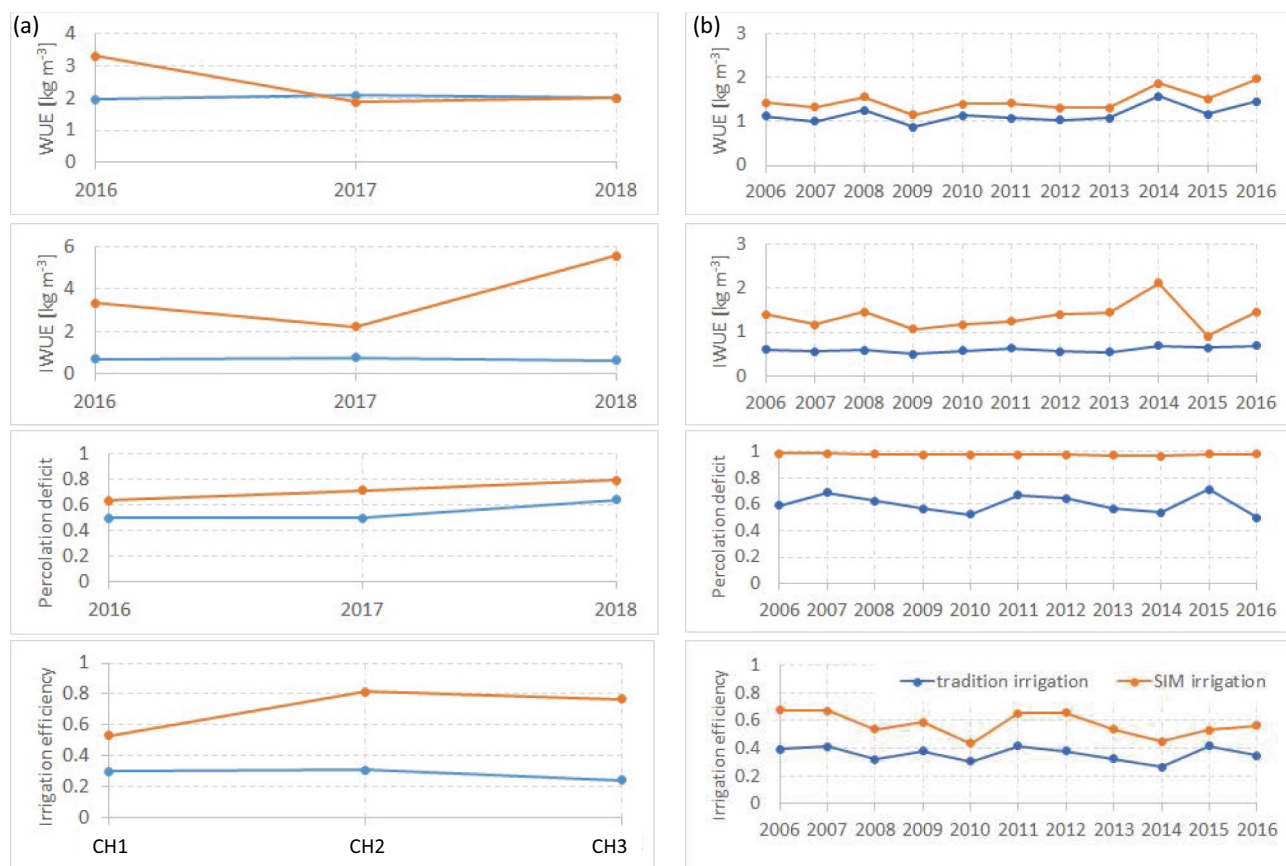
Fig. 10 Water indicators (WUE, IWUE, Percolation deficit, Irrigation efficiency) considering the observed irrigations and the SIM strategy for the analysed maize fields (**a**) and for the whole Chiese Consortium (**b**)

their influence on evapotranspiration computation and which are mainly provided to field scale only or aggregated areal values (Vuolo et al. 2015; Calera Belmonte et al. 2017). Moreover, these methods are usually based on the retrieval of crop parameters (e.g., the crop coefficient) from remote sensing data (D'Urso 2010), while the implemented methodology uses the energy–water balance scheme based on LST. Moreover, the SIM strategy, based on the control of soil moisture, has a higher potential than the strategy based on potential evapotranspiration (D'Urso 2010; Calera Belmonte et al. 2005) due to the possibility of guaranteeing the correct amount of irrigation by also considering acceptable stress conditions for some types of crops in specific growth periods (Zhang et al. 2017). However, a point worth discussing may be represented by the uncertainty embedded in the definition of this soil moisture stress threshold, which is linked to the definition of the p value (Allen et al. 1998). A less precise definition of the triggering threshold could lead to the definition of different irrigation triggering timings and therefore water volumes.

The results found in this study are consistent with previous studies that demonstrated the need for a multi-objective

calibration based not only on local ground measurements but also on distributed information. In particular, Corbari and Mancini (2014), Corbari et al. (2015) and Corbari et al. (2019b) used remotely sensed LST for calibrating the parameters of the FEST-EWB energy–water balance model, showing its potential with respect to the traditional calibration with ground river discharge data. Even though little effort has been made in this direction, some examples are available. Among them, Crow et al. (2003) showed that a calibration based on discharge and land surface temperature improves the estimates of monthly evapotranspiration with respect to a calibration based only on discharge. Instead, Immerzeel and Droogers (2008) demonstrated that good results can be obtained if the calibration of a hydrological model is performed against evapotranspiration maps from a simplified energy balance model.

Conclusion

A methodology for optimizing irrigation volumes at the field and irrigation consortium scales was developed, demonstrating the potential for the combined use of satellite

data and a distributed energy water balance model to estimate soil moisture as a direct regulator of irrigation triggering with respect to crop stress thresholds. The implemented SIM strategy may allow irrigation water volume and the number of irrigations to be conserved with respect to traditional irrigation practices, where farmers tend to over-irrigate, mainly due to the lack of available information on soil moisture dynamics and climate as well as the low water price, which does not motivate farmers to adopt water-saving strategies.

Considerable differences were found in terms of irrigation volume decreases between the northern and southern consortia due to the differences in climate and agricultural practices. An average savings of 500 mm of irrigation water in one season might be obtained when adopting the SIM strategy in the Capitanata Consortium, while an average savings up to 1200 mm could be obtained if the strategy were applied. These results are reflected in an increase of 35% in the IWUE for the tomato fields in the Capitanata Consortium if the SIM strategy had been applied and an increase of approximately 80% for the maize fields in the Chiese Consortium. Instead, the WUE indicator remains almost constant, not changing the evapotranspiration. Instead, higher improvements in irrigation efficiency and percolation deficit are obtained for the Chiese Consortium than for the Capitanata Consortium due to the higher amounts of water, which are traditionally used in excess in northern Italy, independent of the precipitation amount.

The performed analysis relies on a calibrated FEST-EWB model through a pixel-by-pixel procedure based on satellite LST, with absolute errors of 2.5 and 3.4 °C for the Capitanata and Chiese Irrigation Consortia, respectively. The FEST-EWB model was validated locally against soil moisture and evapotranspiration data, reporting RMSE values of approximately 0.07 and 43 Wm^{-2}, respectively.

These results would be helpful to farmers and Water Authorities to comply with European regulations, such as the EU Water Framework Directive 2000/60 and Common Agricultural policy (CAP), which have as objectives the increase of irrigation water use efficiency.

A further improvement of the FEST-EWB model for its use in irrigation management might be the direct accounting of crop growth dynamics to evaluate the effect of water savings on crop yield.

Declarations

References

Acosta-Motos JR, Ortuño MF, Bernal-Vicente A, Diaz-Vivancos P, Sanchez-Blanco MJ, Hernandez JA (2017) Plant responses to salt stress: adaptive mechanisms. Agron 7:18. https://doi.org/10.3390/agronomy7010018

Alexandratos et al (2012) World agriculture towards 2030/2050: the 2012 revision. ESA Working Paper No. 12-03

Allen RG, Pereira LS, Raes D, Smith M (1998) Crop evapotranspiration—guidelines for computing crop water requirements. FAO Irrigation and drainage paper 56, FAO, Rome, Italy, p 300. http://www.fao.org/docrep/x0490e/x0490e00.htm

Bastiaanssen WGM, Steduto P (2017) The water productivity score (WPS) at global and regional level: Methodology and first results from remote sensing measurements. Sci Total Environ 575:595–611. https://doi.org/10.1016/j.scitotenv.2016.09.032

Bastiaanssen WGM, Molden DJ, Makin JW (2000) Remote sensing for irrigated agriculture: examples from research and possible applications. Agric Water Manage 46:137–155. https://doi.org/10.1016/S0378-3774(00)00080-9

Brown PD, Cochrane TA, Krom TD (2010) Optimal on-farm irrigation scheduling with a seasonal water limit using simulated annealing. Agr Water Manage 97:892–900. https://doi.org/10.1016/j.agwat.2010.01.020

Cabelguenne M, Debaeke PH, Puech J, Bosc N (1997) Real time irrigation management using the EPIC – PHASE model and weather forecasts. Agr Water Manage 32:227–238

Calera Belmonte A, Jochum AM, Cuesta GarcÍa A, Montoro Rodríguez A, López Fuster P (2005) Irrigation management from space: towards user-friendly products. Irrig Drain Syst 19:337–353. https://doi.org/10.1007/s10795-005-5197-x

Calera Belmonte A, Campos I, Osann A, D'Urso G, Menenti M (2017) Remote sensing for crop water management: from ET modelling to services for the end users. Sensors 17:1104. https://doi.org/10.3390/s17051104

Cao J, Tan J, Cui Y, Luo Y (2019) Irrigation scheduling of paddy rice using short-term weather forecast data. Agr Water Manage 213:714–723. https://doi.org/10.1016/j.agwat.2018.10.046

Choudhury BJ (1987) Relationships between vegetation indices, radiation absorption, and net photosynthesis evaluated by a sensitivity analysis. Remote Sens Environ 22:209–233. https://doi.org/10.1016/0034-4257(87)90059-9

Comas LH, Trout TJ, DeJonge KC, Zhang H, Gleason SM (2019) Water productivity under strategic growth stage-based deficit irrigation in maize. Agr Water Manage 212:433–440. https://doi.org/10.1016/j.agwat.2018.07.015

Ceppi A, Ravazzani G, Corbari C, Salerno R, Meucci S, Mancini M (2014) Real time drought forecasting system for irrigation management. Hydrol Earth Syst Sci 18:3353–3366. https://doi.org/10.5194/hess-18-3353-2014

Corbari C, Ravazzani G, Mancini M (2011) A distributed thermodynamic model for energy and mass balance computation: FEST-EWB. Hydrol Process 25:1443–1452. https://doi.org/10.1002/hyp.7910

Corbari C, Masseroni D, Mancini M (2012) Effetto delle correzioni dei dati misurati da stazioni eddy covariance sulla stima dei flussi evapotraspirativi. Ital J Agrometeorol 1:35–51

Corbari C, Sobrino JA, Mancini M, Hidalgo V (2013) Mass and energy flux estimates at different spatial resolutions in a heterogeneous area through a distributed energy–water balance model and remote-sensing data. Int J Remote Sens 34:3208–3230. https://doi.org/10.1080/01431161.2012.716924

Corbari C, Mancini M (2014) Calibration and validation of a distributed energy water balance model using satellite data of land surface temperature and ground discharge measurements. J Hydrometeorol 15:376–392. https://doi.org/10.1175/JHM-D-12-0173.1

Corbari C, Bissolati M, Mancini M (2015) Multi-scales and multi-satellites estimates of evapotranspiration with a residual energy balance model in the Muzza agricultural district in Northern Italy. J Hydrol 524:243–254. https://doi.org/10.1016/j.jhydrol.2015.02.041

Corbari C, Salerno R, Ceppi A, Telesca V, Mancini M (2019a) Smart irrigation forecast using satellite LANDSAT data and meteo-hydrological modelling. Agric Water Manag 212:283–294. https://doi.org/10.1016/j.agwat.2018.09.005

Corbari C, Huber C, Yesou H, Huang Y, Su Z, Mancini M (2019b) Multi-Satellite Data of Land Surface Temperature, Lakes Area, and Water Level for Hydrological Model Calibration and Validation in the Yangtze River Basin. Water 11:2621. https://doi.org/10.3390/w11122621

Corbari C, Skokovic D, Nardella L, Sobrino J, Mancini M (2020) Evapotranspiration estimates at high spatial and temporal resolutions from an energy-water balance model and satellite data in the capitanata irrigation consortium. Remote Sens 12:4083. https://doi.org/10.3390/rs12244083

Crow WT, Wood EF, Pan M (2003) Multi-objective calibration of land surface model evapotranspiration predictions using streamflow observations and spaceborne surface radiometric temperature retrievals. J Geophys Res Atmos 108:4725. https://doi.org/10.1029/2002JD003292

Detto M, Montaldo N, Albertson JD, Mancini M, Katul G (2006) Soil moisture and vegetation controls on evapotranspiration in a heterogeneous Mediterranean ecosystem on Sardinia, Italy. Water Resour Res 42:W08419. https://doi.org/10.1029/2005WR004693

D'Urso G (2010) Current status and perspectives for the estimation of crop water requirements from earth observation. Ital J Agron 5:107–120

FAO (2018) The state of food and agriculture. Italy, Rome

Farré I, Faci JM (2009) Deficit irrigation in maize for reducing agricultural water use in a Mediterranean environment. Agr Water Manage 96:383–394. https://doi.org/10.1016/j.agwat.2008.07.002

Foken T (2008) Micrometeorology. Springer, Berlin/Heidelberg, Germany

Geerts S, Raes D (2009) Deficit irrigation as an on-farm strategy to maximize crop water productivity in dry areas. Agric Water Manag 96(9):1275–1284. https://doi.org/10.1016/j.agwat.2009.04.009

Gutman G, Ignatov A (1998) The derivation of the green vegetation fraction from NOAA/AVHRR data for use in numerical weather prediction models. Int J Remote Sens 19:1533–1543. https://doi.org/10.1080/014311698215333

Hatfield JL, Dold C (2019) Water-use efficiency: advances and challenges in a changing climate. Front Plant Sci 10:103. https://doi.org/10.3389/fpls.2019.00103

Immerzeel WW, Droogers P (2008) Calibration of a distributed hydrological model based on satellite evapotranspiration. J Hydrol 349:411–424. https://doi.org/10.1016/j.jhydrol.2007.11.017

Ingram J (2011) A food systems approach to researching food security and its interactions with global environmental change. Food Secur 3:417–431. https://doi.org/10.1007/s12571-011-0149-9

Jimenez-Munoz JC, Sobrino JA, Skokovic D, Mattar C, Cristobal J (2014) Land surface temperature retrieval methods from landsat-8 thermal infrared sensor data. IEEE Geosci Remote Sens Lett 11:1840–1843. https://doi.org/10.1109/LGRS.2014.2312032

Knipper KR, Kustas WP, Anderson MC, Alfieri JG, Prueger JH, Hain C, Gao FN, Yang Y, McKee LG, Nieto H, Hipps L, Aisha M, Sanchez L (2019) Evapotranspiration estimates derived using thermal-based satellite remote sensing and data fusion for irrigation management in California vineyards. Irrig Sci 37:431–449. https://doi.org/10.1007/s00271-018-0591-y

Koech R, Langat P (2018) Improving irrigation water use efficiency: a review of advances, challenges and opportunities in the Australian context. Water 10:1771. https://doi.org/10.3390/w10121771

Kustas W, Norman J, Anderson M, French A (2003) Estimating sub-pixel surface temperatures and energy fluxes from the vegetation index—radiometric temperature relationship. Remote Sens Environ 85:429–440. https://doi.org/10.1016/S0034-4257(03)00036-1

Liang S (2001) Narrowband to broadband conversions of land surface albedo I: algorithms. Remote Sens Environ 76(2):213–238

Lorite IJ, Ramírez-Cuesta JM, Cruz-Blanco M et al (2015) Using weather forecast data for irrigation scheduling under semi-arid conditions. Irrig Sci 33:411–427. https://doi.org/10.1007/s00271-015-0478-0

Mancini M (1990) La Modellazione Distribuita della Risposta Idrologica: Effetti della Variabilità Spaziale e della Scala di Rappresentazione del Fenomeno Dell'assorbimento. Ph.D. Thesis, Politecnico di Milano, Milan, Italy, (In Italian)

Mancini M, Corbari C, Ceppi A, Lombardi G, Ravazzani G, Ben Charfi I, Paciolla N, Cerri L, Sobrino J, Skokovic D, Jia L, Zheng C, Hu G, Menenti M, Herrero Huerta M, Salerno R, Perotto A, Romero R, Amengual A, Hermoso Verger A, Meucci S, Maiorano C, Branca G, Benedetti I, Zucaro R (2021) The SIM operative system for real-time smart irrigation monitoring and forecasting. In preparation

Masseroni D, Corbari C, Mancini M (2014) Limitations and improvements of the energy balance closure with reference to experimental data measured over a maize field. Atmósfera 27(4):335–352. https://doi.org/10.1016/S0187-6236(14)70033-5

Myneni RB et al (2002) Global products of vegetation leaf area and fraction absorbed PAR from year one of MODIS data. Remote Sens Environ 83(1–2):214–231. https://doi.org/10.1016/S0034-4257(02)00074-3

Navarro-Hellín H, Torres-Sánchez R, Soto-Valles F, Albaladejo-Pérez C, López-Riquelme JA, Domingo-Miguel R (2015) A wireless sensors architecture for efficient irrigation water management. Agr Water Manage 151:64–74. https://doi.org/10.1016/j.agwat.2014.10.022

Pelosi A, Medina H, Villani P, D'Urso G, Chirico GB (2016) Probabilistic forecasting of reference evapotranspiration with a limited area ensemble prediction system. Agric Water Manag 178:106–118. https://doi.org/10.1016/j.agwat.2016.09.015

Prueger JH, Parry CK, Kustas WP, Alfieri JG, Alsina MA, Nieto H, Wilson TG, Hipps LE, Anderson MC, Hatfield JL, Gao F, McKee LG, McElrone AJ, Agam N, Los S (2018) Crop water stress index of an irrigated vineyard in the central valley of California. Irrig Sci 37(3):297–313. https://doi.org/10.1007/s00271-018-0598-4

Rawls WJ, Brakensiek DL (1985) Prediction of Soil water properties for hydrologic modelling. Watershed management in the eighties. ASCE, Reston VA USA, pp 293–299

Singh R, Singh GS (2017) Traditional agriculture: a climate-smart approach for sustainable food production. Energ Ecol Environ 2:296–316. https://doi.org/10.1007/s40974-017-0074-7

Skokovic D (2017) Calibration and validation of thermal infrared remote sensing sensors and land/sea surface temperature algorithms over the Iberian Peninsula. Ph.D. Thesis, Universidad de Valencia, Valencia, Spain

Skokovic D, Sobrino JA, Jimenez-Munoz JC (2017) Vicarious calibration of the landsat 7 thermal infrared band and LST algorithm validation of the ETM+ instrument using three global atmospheric profiles. IEEE Trans Geosci Remote Sens 55:1804–1811. https://doi.org/10.1109/TGRS.2016.2633810

Steduto P, Hsiao TC, Raes D, Fereres E (2009) AquaCrop-The FAO crop model to simulate yield response to water: I. Concepts and underlying. Agron J 101(3):426–437. https://doi.org/10.2134/agronj2008.0139s

Taylor KE (2001) Summarizing multiple aspects of model performance in a single diagram. J Geophys Res 106:7183–7192

Toureiro C, Serralheiro R, Shahidian S, Sousa A (2017) Irrigation management with remote sensing: evaluating irrigation requirement for maize under Mediterranean climate condition. Agr Water Manage 184:211–220. https://doi.org/10.1016/j.agwat.2016.02.010

Twine TE, Kustas WP, Norman JM (2000) Correcting eddy-covariance flux underestimates over a grassland. Agri for Meteorol 103:279–300. https://doi.org/10.1016/S0168-1923(00)00123-4

Vuolo F, D'Urso G, De Michele C, Bianchi B, Cutting M (2015) Satellite-based irrigation advisory services: a common tool for different experiences from Europe to Australia. Agric Water Manag 147:82–95. https://doi.org/10.1016/j.agwat.2014.08.004

Wada Y, van Beek LPH, Bierkens MFP (2011) Modelling global water stress of the recent past: on the relative importance of trends in water demand and climate variability. Hydrol Earth Syst Sci 15:3785–3808. https://doi.org/10.5194/hess-15-3785-2011

Xu X, Jiang Y, Liu M, Huang Q, Huang G (2019) Modeling and assessing agro-hydrological processes and irrigation water saving in the middle Heihe River basin. Agr Water Manage 211:152–164. https://doi.org/10.1016/j.agwat.2018.09.033

Zhang H, Xiong Y, Huang H, Xu X, Huang Q (2017) Effects of water stress on processing tomatoes yield, quality and water use efficiency with plastic mulched drip irrigation in sandy soil of the Hetao Irrigation District. Agr Water Manage 179:205–214. https://doi.org/10.1016/j.agwat.2016.07.022

Zucaro R (2014) Atlas of Italian irrigation systems. INEA, Rome, Italy

Zwart SJ, Bastiaanssen WGM, de Fraiture C, Molden DJ (2010) A global benchmark map of water productivity for rainfed and irrigated wheat. Agric Water Manag 97(10):1617–1627. https://doi.org/10.1016/j.agwat.2010.05.018